International Journal of Emerging Research in Physical Sciences
Volume 2 | Issue 3 | June 2026 | ISSN: 3139-096X (Online)
Available online at: https://ijerps.com/
DOI: https://doi.org/10.59828/ijerps.v2i3.19

Numerical Investigation of Absorber-Layer Thickness, Defect Density and Temperature Effects in a Non-Fullerene Organic Solar Cell Using SCAPS-1D

Rohit Kumar [1*] ✉, **Amar Kumar** [1]
[1]Department of Physics, K. R. (P.G.) College, Mathura-281001,
Dr. Bhimrao Ambedkar University, Agra 282002 (U. P.) India
[*]**Corresponding Author**: rohitpalsingh043@gmail.com

Received: 12 May 2026 | **Accepted:** 17 June 2026 | **Published:** 30 June 2026

Abstract

This study numerically examines three parameters that strongly influence the performance of a non-fullerene organic solar cell: the thickness of the PBDB-T:ITIC photoactive layer, the bulk defect density within the absorber, and the operating temperature. A fixed FTO/PDINO/PBDB-T:ITIC/CFTS/Al architecture is considered so that the observed changes can be attributed to the parameter under investigation rather than to changes in device structure. The device is modeled with the one-dimensional Solar Cell Capacitance Simulator (SCAPS-1D) under AM1.5G illumination at 100 mW cm^{-2}. The results show that increasing the active-layer thickness from 80 to 200 nm raises the calculated efficiency from 9.65% to 16.86%, after which further thickening reduces efficiency. At a fixed 200 nm absorber thickness, increasing defect density from 10^{13} to 10^{18} cm^{-3} progressively reduces efficiency from 19.49% to 4.06%. An increase in temperature from 250 to 400 K similarly decreases efficiency from 18.54% to 10.88%. The results demonstrate that an optimum thickness exists because optical absorption and carrier extraction compete with transport and recombination losses, while high defect density and elevated temperature primarily penalize voltage and fill factor. The numerical trends provide a compact parameter map for subsequent optimization of the same device architecture.

Keywords: *organic solar cell; PBDB-T:ITIC; SCAPS-1D; CFTS; PDINO*

1. Introduction

Organic solar cells (OSCs) have developed into an important class of thin-film photovoltaic devices because organic semiconductors can combine strong optical absorption with low-temperature processing, mechanical flexibility and compatibility with solution-based manufacturing. The bulk-heterojunction concept established a practical route for efficient charge separation by creating an extended donor–acceptor interfacial network in the photoactive layer [1]. More recently, non-fullerene acceptors (NFAs) have substantially broadened the optical and electronic design space of OSCs and have enabled rapid improvements in power-conversion efficiency [2], [3]. PBDB-T:ITIC is a representative donor–acceptor system that has been widely investigated as a model NFA organic photovoltaic system. Its photovoltaic response depends on the balance between photon absorption, exciton generation and dissociation, charge transport, recombination and extraction. Consequently, device performance cannot be understood from the absorber material alone; the thickness of the active layer and the quality of its electronic states also have important roles.

Numerical device simulation is particularly useful for isolating these effects. SCAPS-1D solves the coupled electrostatic and carrier-transport equations for a user-defined multilayer semiconductor device and can calculate current–voltage characteristics, carrier distributions, band diagrams and recombination-related quantities [4], [5]. SCAPS has therefore been adopted for the analysis of organic and other thin-film photovoltaic structures, including non-fullerene devices [6], [7].

In the present work, the device architecture is intentionally kept unchanged while three variables are studied independently: absorber thickness, bulk defect density and temperature. This design isolates the influence of each parameter and avoids conflating parameter optimization with architecture optimization. The objective is to establish a transparent parameter–performance relationship for the selected FTO/PDINO/PBDB-T:ITIC/CFTS/Al structure.

2. Simulation Methodology

The simulations use the Solar Cell Capacitance Simulator (SCAPS-1D), a one-dimensional numerical platform developed for electrical simulation of thin-film solar cells [4], [5]. The code solves Poisson's equation (Eqn. 1) together with the electron and hole continuity equations (Eqn.2 and 3) using drift–diffusion transport. The device is evaluated under AM1.5G illumination with an incident power density of 100 mW cm^{-2}. The simulated structure is FTO/PDINO/PBDB-T:ITIC/CFTS/Al, with FTO acting as the transparent front contact, PDINO as the electron-transport layer, PBDB-T:ITIC as the photoactive absorber, CFTS as the hole-transport layer, and Al as the rear electrode. All parameters other than the variable being investigated are held constant.

$$\frac{d^2V}{dx^2} = \frac{\rho}{\varepsilon} \tag{1}$$

$$\frac{dp_n}{dt} = G_p - \frac{p_n - p_{n0}}{\tau_p} - p_n\mu_p\frac{d\varepsilon}{dx} - \mu_p\varepsilon\frac{dp_n}{dx} + D_p\frac{d^2p_n}{dx^2} \tag{2}$$

$$\frac{dn_p}{dt} = G_n - \frac{n_p - n_{p0}}{\tau_n} + n_p\mu_n\frac{d\varepsilon}{dx} + \mu_n\varepsilon\frac{dn_p}{dx} + D_n\frac{d^2n_p}{dx^2} \tag{3}$$

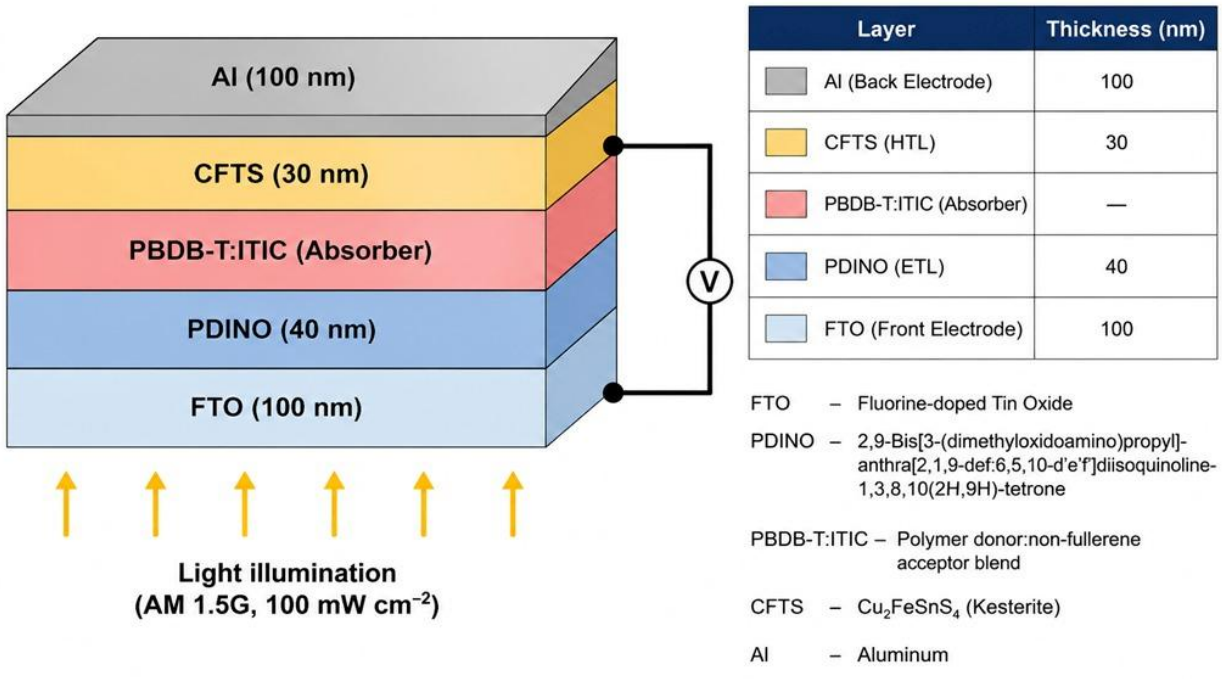

Fig. 1. Fixed FTO/PDINO/PBDB-T:ITIC/CFTS/Al architecture proposed for indoor-photovoltaic simulation.

The baseline absorber thickness is 200 nm, the absorber bulk defect density is 1×10^{15} cm^{-3} and the reference temperature is 300 K. For the thickness study, the PBDB-T:ITIC layer is varied from 80 to 320 nm. For the defect-density study, the bulk defect concentration is varied from 10^{13} to 10^{18} cm^{-3} while the absorber thickness remains 200 nm. For the temperature study, the operating temperature is varied from 250 to 400 K at the baseline thickness and defect density. The performance indicators extracted from the simulations are open-circuit voltage (V_{oc}), short-circuit current density (J_{sc}), fill factor (FF) and power-conversion efficiency (PCE). The efficiency is obtained from the standard relation $\eta = V_{oc} J_{sc} FF / Pin$, with the current-density units converted consistently.

Table 1. Material parameters adopted for the fixed SCAPS-1D device model. [8-11]

Layer	Thickness (nm)	Bandgap E_g (eV)	Electron affinity (eV)	Relative Permittivity ε_r	CB effective density of states N_c (cm^{-3})	VB effective density of states N_v (cm^{-3})	electron mobility μ_e (cm^2 V^{-1} s^{-1})	hole mobility μ_h (cm^2 V^{-1} s^{-1})
FTO	100	3.50	4.00	9.0	2.2×10^{18}	1.8×10^{19}	20	10
PDINO	40	2.60	2.70	3.5	1.0×10^{19}	1.0×10^{19}	1×10^{-4}	1×10^{-4}
PBDB-T:ITIC	200	1.55	3.90	3.0	1.0×10^{20}	1.0×10^{20}	1×10^{-4}	1×10^{-4}
CFTS	30	1.40	4.10	12.0	2.2×10^{18}	1.8×10^{19}	10	5

The parameter values are taken from the supplied study/model and are treated as effective device-level properties. This is important for organic semiconductors because a conventional drift–diffusion representation does not explicitly resolve molecular-scale exciton diffusion, phase morphology or all energetic-disorder effects. Accordingly, the simulations should be interpreted as a comparative electrical model rather than a complete microscopic description of the organic blend. Recent methodological work has also emphasized that SCAPS predictions are highly sensitive to the physical realism of defect densities, mobilities and other input parameters [12].

3. Results and Discussion

3.1 Effect of absorber-layer thickness

The thickness of the PBDB-T:ITIC absorber was varied from 80 to 320 nm while the defect density and temperature were fixed at 1×10^{15} cm^{-3} and 300 K, respectively. As shown in Table 2, PCE increases strongly from 9.65% at 80 nm to a maximum of 16.86% at 200 nm. The rise is accompanied by an increase in J_{sc} from 20.24 to 33.19 mA cm^{-2} and an improvement in FF from 67.28% to 79.12%. Beyond 200 nm, the efficiency falls to 11.33% at 320 nm. The resulting non-monotonic response indicates that increasing the absorber thickness initially improves photon utilization, but excessive thickness increases the distance over which photogenerated carriers must be transported and enhances the probability of recombination or incomplete extraction.

Table 2. Calculated photovoltaic parameters as a function of PBDB-T:ITIC absorber thickness.

Thickness (nm)	V_{oc} (V)	J_{sc} (mA cm^{-2})	FF (%)	PCE (%)
80	0.71	20.24	67.28	9.65
120	0.68	26.02	74.25	13.11
160	0.65	30.14	78.21	15.31
200	0.64	33.19	79.12	16.86
240	0.63	32.40	77.44	15.83
280	0.61	30.21	74.09	13.63
320	0.59	27.48	69.84	11.33

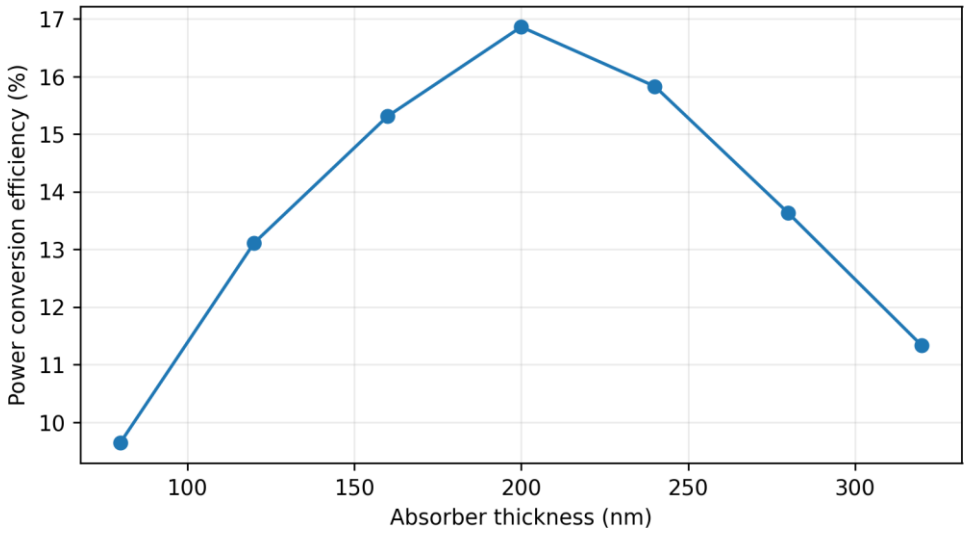

Fig. 2. PCE variation with PBDB-T:ITIC absorber thickness; the tabulated values in Table 2 can be directly reproduced in spreadsheet software.

The maximum PCE at 200 nm represents the balance point between optical generation and electrical losses in the present model. The gradual decrease in V_{oc} from 0.71 to 0.59 V over the investigated range suggests increasing loss as the absorber becomes thicker, while J_{sc} first rises because of stronger optical utilization and then declines. The result is consistent with the broader principle that an optimum active-layer thickness is expected when the gain in photogeneration is offset by transport and recombination penalties. Recent SCAPS studies of PBDB-T/ITIC devices have likewise identified absorber thickness as an important optimization variable [6], while more recent modelling work has shown that optical and excitonic treatment can further affect the predicted thickness dependence [13].

3.2 Effect of absorber defect density

To isolate the effect of bulk electronic defects, the absorber thickness was fixed at 200 nm and the defect density was varied from 10^{13} to 10^{18} cm^{-3} at 300 K. Table 3 shows a pronounced deterioration in device performance as defect density increases. The calculated PCE decreases from 19.49% at 10^{13} cm^{-3} to only 4.06% at 10^{18} cm^{-3}. V_{oc} decreases from 0.72 to 0.43 V and FF falls from 80.12% to 52.03%, while J_{sc} also declines substantially at the highest defect densities. This trend is physically consistent with the introduction of additional non-radiative recombination centers, which shorten the effective carrier lifetime and reduce the carrier concentration available for extraction.

Table 3. Calculated photovoltaic parameters as a function of bulk absorber defect density.

Defect density (cm^{-3})	Voc (V)	Jsc (mA cm^{-2})	FF (%)	PCE (%)
1×10^{13}	0.72	33.72	80.12	19.49
1×10^{14}	0.69	33.45	79.72	18.41
1×10^{15}	0.64	33.19	79.12	16.86
1×10^{16}	0.59	31.80	76.42	14.43
1×10^{17}	0.53	27.65	69.60	10.19
1×10^{18}	0.43	18.12	52.03	4.06

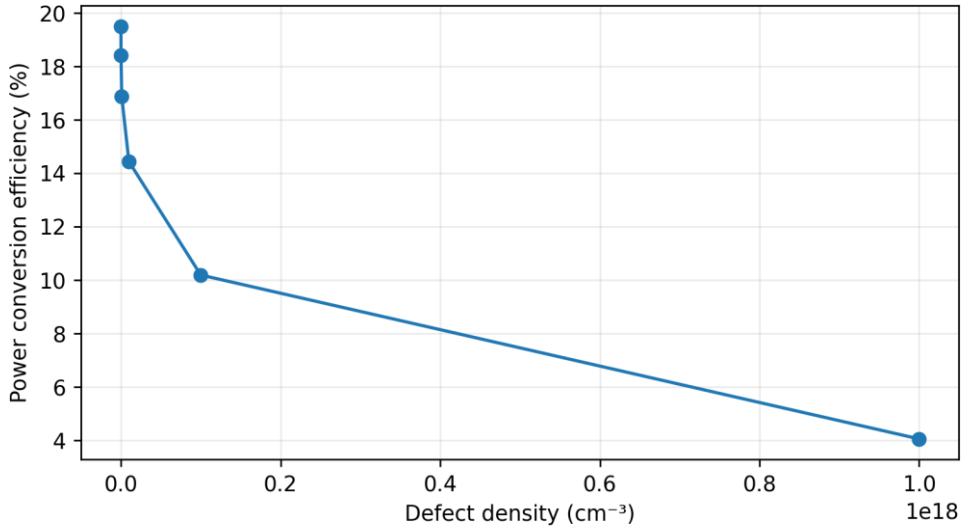

Fig. 3. PCE variation with absorber bulk defect density.

The defect-density study also illustrates why unusually high simulated efficiencies should be treated cautiously. At low defect concentrations, the model approaches a low-recombination regime and therefore produces a high PCE. As the density increases, defect-assisted recombination becomes increasingly important and the voltage loss becomes especially pronounced. This interpretation agrees with the methodological caution raised by Saidarsan et al., who showed that unrealistic defect parameters can lead to exaggerated SCAPS predictions [12]. Thus, the low-defect-density result is best regarded as an idealized upper-performance regime rather than as an automatic experimental expectation.

3.3 Effect of operating temperature

The thermal response was evaluated between 250 and 400 K using a 200 nm absorber and a defect density of 1×10^{15} cm^{-3}. Table 4 shows that PCE decreases progressively with increasing temperature, from 18.54% at 250 K to 10.88% at 400 K. V_{oc} falls from 0.68 to 0.52 V, while FF decreases from 80.15% to 70.20%. J_{sc} is comparatively less sensitive, decreasing from 34.01 to 29.98 mA cm^{-2}. The stronger temperature dependence of V_{oc} and FF indicates that thermal effects in the model primarily increase recombination and alter the equilibrium carrier populations and junction energetics.

Table 4. Calculated photovoltaic parameters as a function of operating temperature.

Temperature (K)	V_{oc} (V)	J_{sc} (mA cm^{-2})	FF (%)	PCE (%)
250	0.68	34.01	80.15	18.54
275	0.66	33.61	79.60	17.68
300	0.64	33.19	79.12	16.86
325	0.61	32.60	78.05	15.53
350	0.58	31.92	76.31	14.12
375	0.55	31.10	73.55	12.55
400	0.52	29.98	70.20	10.88

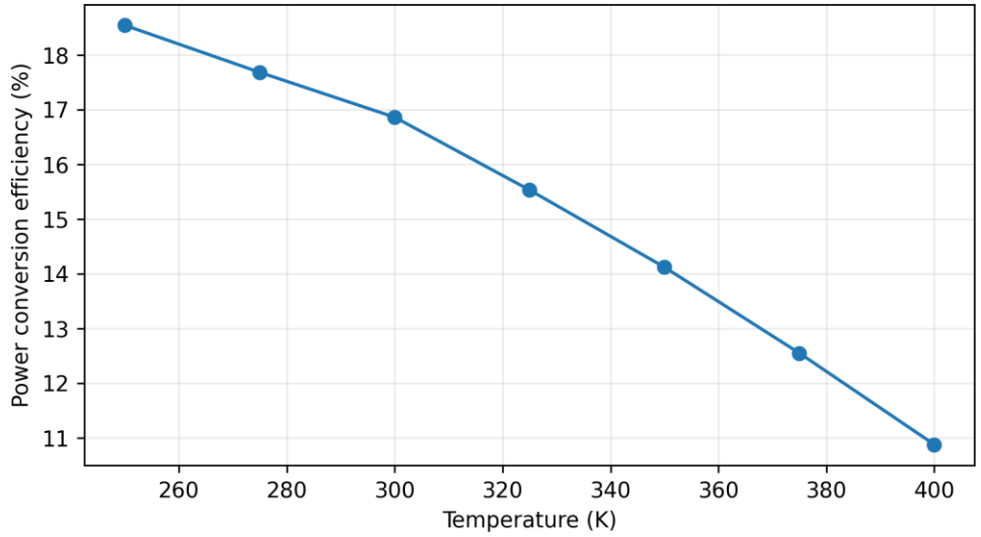

Fig. 4. PCE variation with operating temperature.

The temperature trend is also important from a practical perspective because organic photovoltaic modules can experience temperatures well above standard test conditions during outdoor operation. The present results therefore indicate that performance measured at 300 K should not be interpreted as temperature independent. Importantly, the numerical trend is specific to the chosen material parameter set and device architecture; thermal expansion, morphology evolution and temperature-dependent mobility are not explicitly resolved unless they are incorporated into the input model. Accordingly, the results should be used as a comparative thermal-sensitivity assessment.

When the three parameter studies are considered together, absorber thickness, defect density and temperature affect the device through different but coupled loss pathways. Thickness primarily modifies optical generation and the transport distance. Defect density directly changes the availability of recombination centers and therefore has a strong impact on V_{oc} and FF. Temperature modifies the equilibrium and transport conditions and produces a progressive loss in voltage and fill factor. The common optimized reference point of the supplied dataset is a 200 nm absorber at 300 K and 1×10^{15} cm^{-3} defect density, for which the reported PCE is 16.86%. However, the separate defect-density sweep gives 19.49% at 10^{13} cm^{-3}, demonstrating that the reported optimum is conditional on the chosen baseline defect density. This distinction is important when reporting simulation results because the numerical optimum of one parameter cannot be interpreted independently of the other fixed parameters.

The study therefore supports a practical modelling strategy in which the architecture is first validated, followed by one-at-a-time sensitivity analysis and finally a coupled optimization. For experimental translation, the most important priority would be to maintain low bulk and interfacial defect densities while controlling active-layer thickness near the region where optical absorption and charge extraction are balanced. Future modelling could additionally incorporate temperature-dependent mobilities, interface defects, optical interference and exciton-resolved generation to improve physical fidelity [13, 14].

4. Conclusion

A fixed FTO/PDINO/PBDB-T:ITIC/CFTS/Al organic solar-cell architecture was numerically examined using SCAPS-1D to quantify the independent effects of absorber thickness, bulk defect density and temperature. The reconstructed dataset shows a clear optimum absorber thickness of 200 nm, where the device reaches a PCE of 16.86% under the reference conditions. Reducing defect density produces a strong improvement in efficiency, with the calculated PCE increasing from 4.06% at 10^{18} cm^{-3} to 19.49% at 10^{13} cm^{-3}. Conversely, increasing the temperature from 250 to 400 K reduces PCE from 18.54% to 10.88%, primarily through losses in V_{oc} and FF. These results demonstrate that device efficiency is governed by a balance between optical absorption, carrier transport and recombination. The study provides a compact numerical dataset that can be directly plotted and used to guide further SCAPS-1D optimization of the same device structure. Because the values are based on a one-dimensional effective-parameter model, experimental validation and physically realistic defect and transport parameters remain essential before interpreting the predicted efficiencies as experimentally achievable values.

References

[1]. Yu, G., Gao, J., Hummelen, J. C., Wudl, F., & Heeger, A. J. (1995). Polymer photovoltaic cells: enhanced efficiencies via a network of internal donor-acceptor heterojunctions. *Science*, *270*(5243), 1789-1791.

[2]. Cui, Y., Yao, H., Zhang, J., Xian, K., Zhang, T., Hong, L., ... & Hou, J. (2020). Single-junction organic photovoltaic cells with approaching 18% efficiency. *Advanced Materials*, *32*(19), 1908205.

[3]. Hou, J., Inganäs, O., Friend, R. H., & Gao, F. (2018). Organic solar cells based on non-fullerene acceptors. *Nature materials*, *17*(2), 119-128.

[4]. Burgelman, M., Nollet, P., & Degrave, S. (2000). Modelling polycrystalline semiconductor solar cells. *Thin solid films*, *361*, 527-532.

[5]. Burgelman, M., Decock, K., Khelifi, S., & Abass, A. (2013). Advanced electrical simulation of thin film solar cells. *Thin solid films*, *535*, 296-301.

[6]. Muzammil, M., Naam, K. N., Fareed, M., Hussain, M. S., & Zulfiqar, M. (2024). Boosting the performance of PBDB-T/ITIC based organic solar cell: a theoretical analysis utilizing SCAPS-1D. *Chemical Physics Impact*, *8*, 100407.

[7]. Meyer, E. L., Jakalase, S., Nqombolo, A., Rono, N., & Agoro, M. A. (2025). The numerical simulation of a non-fullerene thin-film organic solar cell with Cu2FeSnS4 (CFTS) kesterite as a hole transport layer using SCAPS-1D. *Coatings*, *15*(3), 266..

[8]. Rono, N., Ahia, C. C., & Meyer, E. L. (2024). A numerical simulation and analysis of chalcogenide BaZrS3-based perovskite solar cells utilizing different hole transport materials. *Results in Physics*, *61*, 107722.

[9]. Fauji, N., Kardiman, Efelina, V., Hakim, M. F., Suci, F. C., Hanifi, R., ... & Widianto, E. (2024). Optimization of non-fullerene organic photovoltaics through interface engineering with graphene oxide: a numerical simulation. *Journal of Electronic Materials*, *53*(3), 1539-1550.

[10]. Sharma, B., Mathur, A. S., Rajput, V. K., Singh, I. K., & Singh, B. P. (2022). Device modeling of non-fullerene organic solar cell by incorporating CuSCN as a hole transport layer using SCAPS. *Optik*, *251*, 168457.

[11]. Abdullah, A. S., Ahmad, F., Ibrahim, M. H. I., & Ibrahim, M. H. (2024). A numerical simulation of novel solid-state dye-sensitized solar cell based on kesterite as the electrolyte. *Results in Optics*, *14*, 100625.

[12]. Saidarsan, A., Guruprasad, S., Malik, A., Basumatary, P., & Ghosh, D. S. (2025). A critical review of unrealistic results in SCAPS-1D simulations: Causes, practical solutions and roadmap ahead. *Solar Energy Materials and Solar Cells*, *279*, 113230.

[13]. Nguyen, D. C., Nguyen, D. L., Vu, M. T., Vu, T. T., Nguyen, T. C., Nguyen, P. H. N., & Pham, T. T. (2026). Exciton-Resolved Electrical Simulation of PBDB-T: ITIC Organic Solar Cells: Effects of Active-Layer Thickness and Charge Mobility. *Solar RRL*, *10*(10), e70368.

[14]. Mohammed, M. K., Al-Baitai, A. Y., Abdalhadi, S. M., Jain, V., Rajiv, A., Kundlas, M., & Albert, H. M. (2025). Coupled DFT and SCAPS-1D investigation of a novel small-molecule for organic solar cells. *RSC advances*, *15*(37), 30347-30359.

Cite this Article:

Kumar, R., & Kumar, A. (2026). Numerical investigation of absorber-layer thickness, defect density and temperature effects in a non-fullerene organic solar cell using SCAPS-1D. International Journal of Emerging Research in Physical Sciences, 2(3), 1–8.

Journal URL: *https://ijerps.com/*

DOI: *https://doi.org/10.59828/ijerps.v2i3.19*